We are IntechOpen,
the world's leading publisher of
Open Access books
Built by scientists, for scientists

6,900
Open access books available

186,000
International authors and editors

200M
Downloads

Our authors are among the

154
Countries delivered to

TOP 1%
most cited scientists

12.2%
Contributors from top 500 universities

CLARIVATE ANALYTICS
BOOK CITATION INDEX
INDEXED

WEB OF SCIENCE™

Selection of our books indexed in the Book Citation Index
in Web of Science™ Core Collection (BKCI)

Interested in publishing with us?
Contact book.department@intechopen.com

Numbers displayed above are based on latest data collected.
For more information visit www.intechopen.com

Ferroelectric Polymer for Bio-Sonar Replica

Antonino S. Fiorillo and Salvatore A. Pullano
School of Biomedical Engineering, University of Magna Græcia,
Italy

1. Introduction

The sensorial knowledge paradigm has captured the interest of many eminent scholars in past centuries (the philosophical trend of "*Sensism*" was developed around the "*Gnoseologic Paradigm*", which has found its highest expression in Étienne Bonnot de Condillac, 1930) as well as in the modern era, particularly in the attempt to interface the external environment to humans through artificial systems. Of the five human senses, which have been investigated by scientists involved in artificial perception studies, vision, touch and hearing have received the most attention, each one for different reasons. When referring to hearing as the sense which perceives sound (the mechanical perturbation induced in a medium by a travelling wave at suitable frequency), a distinction should be made. Indeed, sound between 100 Hz and 18 kHz refers mainly to the range of human perception, while infrasound (up to 20 or 30 Hz) and low frequency ultrasound (from 20 to 120 kHz) refer to animal (mammalian) perception.

Low frequency ultrasounds have been amply investigated in the last century and the resulting applications have been made in both military and civil fields. In any case, it appears relevant and necessary to improve the performance of the ultrasonic system (more properly named sonar) for use in a variety of industrial, robotic, and medical applications where ranging plays a basilar role. Nevertheless, other important information can be extrapolated through proper use of the ultrasonic signal as is evident from the study of the biology and mammalian behaviour (Altringham, 1996). Up to now, attempts have been made to try to emulate animal auditory systems by using both commercial or custom piezoelectric transducers. In this context, the latest investigation in artificial perception was mainly inspired by bat bio-sonar, which has been extensively studied and described by biologists.

As a result of the damping exerted by the propagation medium, which increases as the ultrasound frequency increases, conventional transducers normally function at relatively low frequencies (40 ÷ 50 kHz) in air. Sometimes this restricts choices of piezoelectric materials, besides transducer shape and dimensions. In order to increase the frequency and hence to improve the performances of ultrasonic transducers, flexible plastic materials, such as the ferroelectric polymer polyvinylidene fluoride (PVDF) were investigated and assembled in different geometries. It was discovered that, when properly shaped, PVDF films can resonate at frequencies superior to 100 kHz, covering the full range frequency of the majority of bat bio-sonars (20 ÷ 120 kHz).

The first part of a work aimed at emulating the auditory system of Pteronotus Parnellii, (also known as the *moustached bat*) is described in this chapter. We have simulated some of this

bat's most important strategies, based on the techniques used by its sophisticated echo-location system in gathering ultrasonic information. Specifically, in this phase of the study, the piezoelectric transducer is used to emulate the function of the bat cochlea in a real distance measurement, although bio-sonar capabilities are far superior.

The chapter is organized as follows: first the design and characterization of the ferroelectric polymer ultrasonic transducer is discussed. Based on the piezoelectric equilibrium rules, a suitable transducer geometry has been designed in order to improve the device's performance in air.

Then the transducer impedance has been characterized from 30 to 40 kHz up to 120 kHz, exactly in the same range frequency in which most bat bio-sonars operate. The design of the electronic circuits and the matching of the electric impedance with the ultrasonic transducer received particular attention because of the inherent noise of the PVDF. The sensory unit operates at distances of 10 ÷ 2500 mm with an axial resolution of about 2 mm down to 500 μm. A critical comparison between the custom transducer (based on ferroelectric polymer technology) and similar devices (based on different, but standard, technologies) is also carried out.

These and other problems are considered in this work, including a neural network approach carried out in order to verify the potentiality of the PVDF electronic sonar and the analogism with the bat bio-sonar, in all its complexity, with the aim of exploring how artificial perception in the acoustic field can support human sensorial perception.

Nomenclature

c	Stiffness coefficient	$[N \cdot m^{-2}]$
d	Piezoelectric constant	$[C \cdot N^{-1}]$
C	Capacitance	$[F]$
D	Normal electric displacement	$[C \cdot m^{-2}]$
e	Piezoelectric constant	$[C \cdot m^{-2}]$
E	Electric field	$[V \cdot m^{-1}]$
f	Frequency	$[Hz]$
g	Piezoelectric constant	$[V \cdot m \cdot N^{-1}]$
h	Piezoelectric constant	$[V \cdot m^{-1}]$
I	Electric current	$[A]$
k	Piezoelectric coupling factor	
L	Inductance	$[H]$
M	Figure of merit	
P	Polarization	$[C \cdot m^{-2}]$
Q	Quality factor	
R	Resistance	$[\Omega]$
r	Bending radius	$[m]$
S	Strain	
s	Elastic compliance	$[m^2 \cdot N^{-1}]$
T	Tangential stress	$[N \cdot m^{-2}]$
β	Dielectric impermeabilities	$[m \cdot F^{-1}]$
ε	Permittivity	$[F \cdot m^{-1}]$
ε_r	Relative permittivity	
ε_0	Vacuum permittivity	$[F \cdot m^{-1}]$

φ	Angle	[deg]
SNR	Signal-to-noise ratio	

2. PVDF transducer analogy to bat cochleas

The auditory system of mammals is characterized by a common basic layout in which one can identify three anatomical regions—the external and middle ears (air filled) and the inner ear (filled with biological fluid). The acoustic waves are received, conveyed, and amplified by the external and middle ears, while the vibrational energy related to sound pressure is converted into bio-electric energy by the inner ear. Sound amplification is carried out mechanically by a system which includes the ossicles: the malleus, the incus, and the stapes; and the eardrum.

In the system we propose for bio-sonar replication, the amplification of the signal and all other steps included in acoustical signal conditioning are carried out electronically, while the piezoelectric transducer is concerned with the conversion of mechanical energy. Our attention was focalized on the third anatomic region, particularly the cochlea, which transduces mechanical energy into bio-electrical energy, and the acoustic nerve, which carries the bio-electrical signal to the cerebral cortex.

In this section the anatomic structure of the cochlea and its working is reviewed in order to clarify and justify the choice concerning materials, particularly the ferroelectric polymer, and methods used to emulate the bio-sonar of bats.

The cochlea of a bat, similar to that of other mammals, boasts a hollow spiral geometry divided into three channels; the vestibular and tympanic channels are filled with endolymph, which is very similar to intracellular liquid, and the middle channel is filled with perilymph, similar to extracellular liquid, each one separated by an endothelial membrane (see Figure 1). As far as the electronic system is concerned, the most important component is the basilar membrane which, through vibration, activates the receptors of the organ of Corti, that lie over it (the organ of Corti includes the tectorial membrane, two different systems of hair cells, and nervous fibres; these generate bio-pulses as a consequence of the vibration).
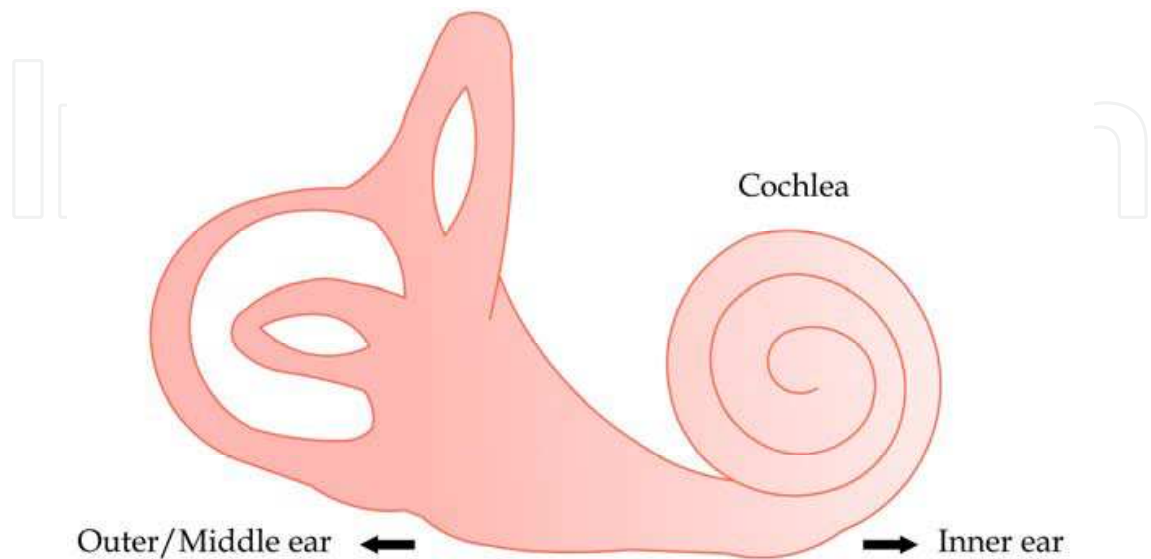

Fig. 1. Main part of the inner ear and arrangement of cochlear component.

When the acoustic wave reaches the eardrum after passing through the outer ear canal, it has already been primarily amplified in this resonant cavity of the external ear. Successively it is mechanically amplified in the middle ear by the chain of ossicles acting as levers on the oval window, located in the inner ear. The travelling wave, once in the cochlea, propagates along the basilar membrane (see Figure 2), which acts as a mechanical filter with respect to the frequency spectrum. Different frequency components of the signal cause the motion of different parts of the membrane in a tonotopic organization. The behaviour of the basilar membrane is related to its geometry, because moving from the base toward the apex the membrane increases its width and thickness, while the resonance frequency decreases.
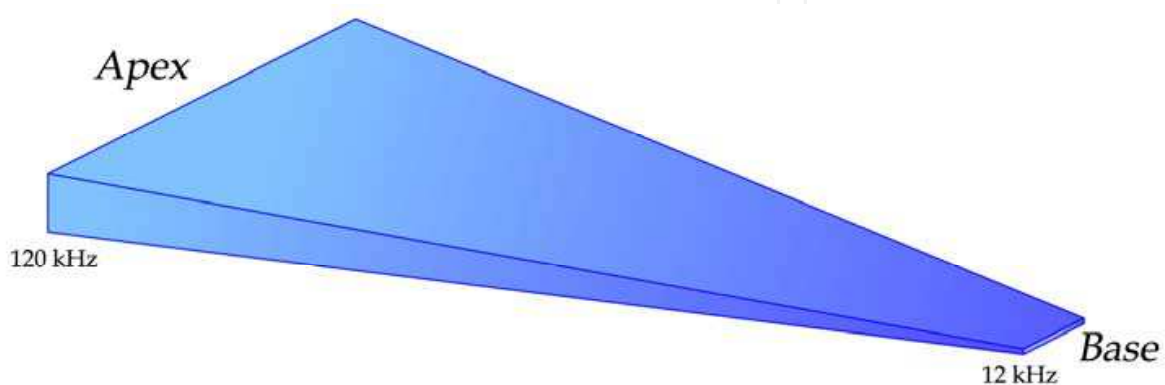

Fig. 2. Basilar membrane winding inside the cochlea

The receptors located in the organ of Corti are divided into outer and inner hair cells, and perform two different functions. The motion of the basilar membrane intimately connected to the organ of Corti is first amplified by the outer hair cells and then transmitted through the liquid to the tectorial membrane that induces the deflection of the hair in the inner cells. The inner hair cells transduce the mechanical signal, after amplification, into an electrochemical signal through the activation of ionic channels and the release of a neurotransmitter (glutamate) to the acoustic nerve, as a consequence of the polarization level of the cells itself. The neurotransmitter reaches the central nervous system through the *afferent fibres*, which account for 90 ÷ 95 % of the total connections, while the rest are connected to the inner hair cells. From the bio-electrical point of view, this process is concerned with the generation of an action potential which drives ionic currents along the axons of the *afferent fibres* (see Figure 3); conversely, the majority of the *efferent fibres* connect the central nervous system to the outer hair cells.

Referring to the analogism with the artificial system, the PVDF ultrasonic transducer acts in a way similar to the basilar membrane, except for the absence of the outer hair cells. In effect though, the acoustic pressure is not mechanically amplified, but merely converted, by the direct piezoelectric effect , into an electrical signal and, hence, only *afferent electronic pathways* are considered. PVDF is a light and flexible plastic material, of several tens of μm in thickness, which can be shaped into hemicylindrical geometries in order to fabricate the ultrasonic transducer which resonates in the frequency range of bat biosonar. The resonance frequency is inversely proportional to the bending radius and can be easily tuned to the suitable values necessary for the specific tasks accomplished by the bat. In fact the curved PVDF ultrasonic transducer works in a way similar to the basilar membrane.
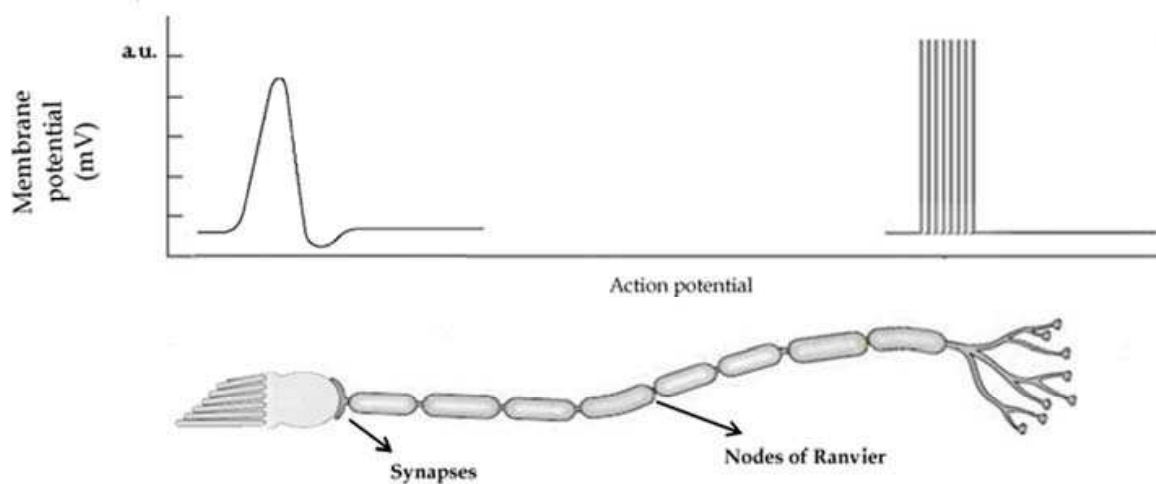
Fig. 3. Structure of hair cell and axon with generated potential along it. The synapses carries the neurotransmitter molecules through the axon. The nodes of Ranvier refresh action potential through the pathway.

The electric dipoles in piezo-polymer, upon the application of an external pressure, generate a net electric charge (which is conveyed through the *afferent electronic pathways* to the central processing system); the inner hair cells also generate a bio-electrical stimulus upon deflection of the basilar membrane. In the next section of this chapter we briefly introduce the ferroelectric phenomenon in PVDF with emphasis on the piezoelectric effect and we describe the design and characterization of the ultrasonic transducer.

3. Polyvinylidene fluoride (PVDF) polymer

To understand the behaviour of ferroelectric materials and their field of application as sensors, we look at both the piezoelectric and pyroelectric effects. Crystals without centers of symmetry may have one or more polar axes and show both vectorial and tensorial properties. Since they exhibit spontaneous polarization, they are defined polar crystals, which display a pyroelectric effect, that is, a change in polarization under a gradient of temperature (Jona & Shirane, 1962; Berlincourt, 1981). In addition, polar crystals exhibit both a direct piezoelectric effect (a state of electrification caused by a mechanical deformation) and a converse piezoelectric effect (a mechanical deformation caused by the exertion of an external electric field) (Curie, 1880). At the end of the 60's, the discovery of strong piezoelectric (Kawai, 1969) and pyroelectric activity (Bergman et al., 1971) in PVDF ascribed the polymer to the family of synthetic ferroelectric polycrystals.

3.1 Atomic structure and morphology

Polyvinylidene fluoride is a semicrystalline linear polymer, with long molecular chains in which each monomer $\left[-CH_2 - CF_2 - \right]$ has a dipole moment. It is synthesized in poly-crystalline forms, the most important of which are the α and β forms shown in Figure 4. In the α form (or form II), obtained by fusion, the lattice has a monoclinic unit cell with 2/m symmetry and contains trans-gauche/trans-gauche molecular conformation (TGTG'). The β form (or form I) is obtained from the α form by low temperature stretching. In this case, the lattice unit cell is orthorhombic with mm2 symmetry and all-trans zigzag molecular

conformation (TTTT). Unlike the α antipolar crystal form, the β form is piezoelectric and exhibits spontaneous polarization. Although there are two other crystalline structures αₚ and γ, for technological purposes the β form is the most interesting due to its stronger piezoelectric and pyroelectric properties (Davis, 1988).
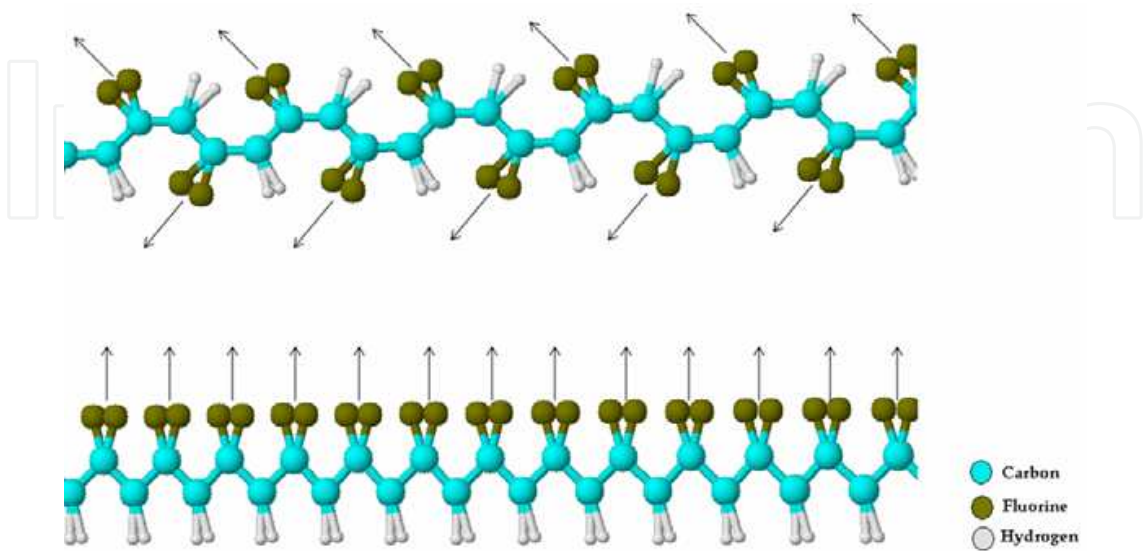

Fig. 4. Representation of crystalline α (upper) and β (lower) forms. Arrows indicate the orientation of the dipole moment.

3.2 Poling methods

Because of its molecular conformation, unoriented PVDF in the α form does not exhibit large piezoelectric and pyroelectric coefficients. In order to induce reproducible ferroelectric characteristics, the polymer must be oriented and poled (a higher degree of orientation results in increased piezoelectric activity). There are several techniques for poling PVDF including: corona poling, thermal poling, plasma and higher electric field poling, and simultaneous poling/stretching techniques. Starting with a non-polar α form, the polymer film is heated to 50 ÷ 60 °C and then uniaxially stretched along direction 1 called the "Machine Direction" or alternatively stretched biaxially along direction 2, called the "Transverse Direction", as shown in Figure 5. Stretching recrystallizes the PVDF in the β form, which renders it suitable to be poled using some of the previously mentioned techniques.
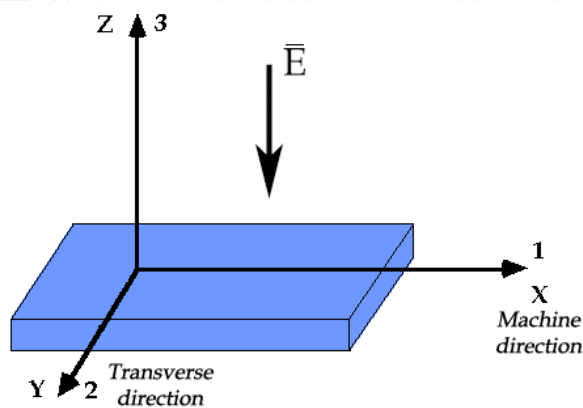

Fig. 5. Fundamental directions of PVDF film

The corona discharge is a room-temperature poling technique accomplished by applying high voltage to the PVDF film, placed between a flat electrode and an array of conductive tips placed at a distance of a few millimeters with an interposed control grid. The poling process is completed within several seconds and a high temperature was found to yield greater and more stable piezoelectric and pyroelectric effects (Bloomfield et al., 1987). Poling can also be carried out by applying electric fields, between 500 kV/cm and 800 kV/cm at high temperatures (90 ÷ 110 °C) for about one hour; the electric fields must be applied directly to both the metalized faces of the film. High temperatures create thermal agitation, allowing a partial alignment of the dipoles due to the electric field. Successively, the temperature is decreased and then the electric field switched off, resulting in a permanently polarized state of the polymer (Hasegawa et al., 1972). One of the most utilized methods (Bauer, 1989) is that of applying an alternating electric field through the polymer at a frequency ranging from 0.001 Hz to 1 Hz, while gradually increasing the amplitude of the electric field, which results an hysteresis loop of polarization. This technique allows the achievement of a very stable, reproducible and durable polarization.

Polarization can easily be controlled by monitoring the actual current passing through the polymer which is given by:

$$i = \varepsilon \left(\frac{dE}{dt} \right) + \left(\frac{dP}{dt} \right) + \left(\frac{E}{R} \right) \tag{1}$$

3.3 Piezoelectric equations

A necessary condition to induce piezoelectricity in a medium is the absence of a center of symmetry in its atomic structure. Starting from thermodynamic potential, in adiabatic and isothermal conditions, general piezoelectric equations can be derived. Neglecting the effects of the magnetic field, the most useful simplified equations are given as follows:

$$
\begin{cases}
S = s^E T + d_t E \\
D = dT + \varepsilon^T E
\end{cases}
$$
$$
\begin{cases}
S = s^D T + g_t D \\
E = -gT + \beta^T D
\end{cases}
$$
$$
\begin{cases}
T = c^D S - h_t D \\
E = -hS + \beta^S D
\end{cases} \tag{2}
$$
$$
\begin{cases}
T = c^E S - \varepsilon_t E \\
D = eS + \varepsilon^S E
\end{cases}
$$

The first pair of equations is the most used, where electric field and stress are taken as independent variables. The second pair of equations can be used for general purposes except for triclinic and monoclinic crystal systems. The last two pairs are used when the strain is prevalent in only one dimension. The four piezoelectric constants are related as follows:

$$d = \frac{\partial S}{\partial E}\bigg|_T = \frac{\partial D}{\partial T}\bigg|_E \qquad g = -\frac{\partial E}{\partial T}\bigg|_D = \frac{\partial S}{\partial D}\bigg|_T \tag{3}$$

$$e = -\frac{\partial T}{\partial E}\bigg|_S = \frac{\partial D}{\partial S}\bigg|_E \qquad h = -\frac{\partial T}{\partial D}\bigg|_S = \frac{\partial E}{\partial S}\bigg|_D$$

Below a brief notation in matrix form of the tensor theory for PVDF is reported (Mason, 1964, 1981):

$$
\begin{vmatrix} S_1 \\ S_2 \\ S_3 \\ S_4 \\ S_5 \\ S_6 \\ D_1 \\ D_2 \\ D_3 \end{vmatrix} =
\begin{vmatrix}
s_{11}^E & s_{12}^E & s_{13}^E & 0 & 0 & 0 & 0 & 0 & d_{31} \\
s_{12}^E & s_{11}^E & s_{13}^E & 0 & 0 & 0 & 0 & 0 & d_{31} \\
s_{13}^E & s_{13}^E & s_{44}^E & 0 & 0 & 0 & 0 & 0 & d_{44} \\
0 & 0 & 0 & s_{44}^E & 0 & 0 & 0 & d_{15} & 0 \\
0 & 0 & 0 & 0 & s_{44}^E & 0 & d_{15} & 0 & 0 \\
0 & 0 & 0 & 0 & 0 & s_{66}^E & 0 & 0 & 0 \\
0 & 0 & 0 & 0 & d_{15} & 0 & \varepsilon_{11}^T & 0 & 0 \\
0 & 0 & 0 & d_{15} & 0 & 0 & 0 & \varepsilon_{11}^T & 0 \\
d_{31} & d_{31} & d_{33} & 0 & 0 & 0 & 0 & 0 & \varepsilon_{33}^T
\end{vmatrix}
\cdot
\begin{vmatrix} T_1 \\ T_2 \\ T_3 \\ T_4 \\ T_5 \\ T_6 \\ E_1 \\ E_2 \\ E_3 \end{vmatrix}
\tag{4}
$$

One of the most important properties of piezoelectric materials is their ability to convert energy, expressed by the piezoelectric coupling factor k which is related to the mutual, elastic, and dielectric energy density. It is a useful parameter for the evaluation of power transduction, and is better than the sets of elastic, dielectric and piezoelectric constants.

4. PVDF applications

4.1 Acoustical and optical devices

The most common applications of PVDF are in the fields of electro-acoustic, electro-mechanic (Sessler, 1981; Lovinger, 1982, 1983; Hunt et al., 1983), and pyroelectric transducers (a "vidicon" imaging system was proposed by Yamaka, 1977). In the field of electroacoustic transducers, the ferroelectric polymer was largely used as an ultrasonic transducer in the MHz frequency range for application in the medical field, and in the audio frequency range. In the first case, its functioning principle is based on the thickness mode of vibration along the z direction (see Figure 5), in which one or both of the wide faces are clamped to a rigid bulk, while in the second case, at much lower frequencies, the transverse piezoelectric effect along the x direction is predominant.

Thanks to its piezoelectric characteristics (compared in Table 1 with other piezoelectric materials such as low Q - quality factor - together with low acoustic impedance, lightness, conformability, and very low cost), it is also a competitive material in the fabrication of ultrasonic transducers. It resonates in the thickness mode at very high frequencies, for use in non-destructive testing in clinical medicine (Ohigashi et al., 1984).

Property	Unit	PZT4	PZT5A	PZT5H	PbNb$_2$O$_6$	PVDF	P(VDF-TrFE)
Sound velocity	m/s	4600	4350	4560	3200	2260	2400
Density	10^{3}kg/m^3	7.5	7.75	7.5	6.2	1.78	1.88
Acoustic impedance	10^{6}Rayl	34.5	33.7	34.2	20	4.2	4.51
Elastic constant	10^{9}N/m	159	159	147	-	9.1	11.3
Electromechanical Coupling Factor k$_{31}$		0.51	0.49	0.50	0.32	0.2	0.3
Piezoelectric constant							
e$_{33}$	C/m^2	15.1	15.8	23.8	-	-0.16	-0.23
h$_{33}$	10^{9}V/m	2.68	2.15	1.84	-	-2.9	-4.3
d$_{33}$	pC/N	289	375	593	85	17.5	18
d$_{31}$	pC/N	-123	-	-	-	25	12.5
g$_{33}$	V·m/N	0.0251	0.0249	0.0197	0.032	-0.32	-0.38
$\varepsilon_r = \varepsilon_{33}/\varepsilon_0$		635	830	1470	300	6.2	6

Table 1. Comparison of main piezomaterial properties

Another high frequency application is in combination with integrated electronic circuits in the fabrication of a 32-element array configuration for ultrasonic imaging (Swartz and Plummer, 1979).

The performance of transducers realized on silicon was improved by spinning a 15 μm-thin layer of a solution of P(VDF-TrFe) (a copolymer of the polyvinylidene fluoride) in MEK (Methyl Ethyl Ketone), onto a processed silicon wafer in which a low noise NMOS transistor with an extended gate was integrated (Fiorillo et al., 1987).

4.2 Low frequency ultrasound devices

At much lower frequencies, an electric potential applied to both of the wide faces of a free PVDF sheet, generates length-extensional vibrations along x that can be converted into a radial vibration by curvature. This second principle of functioning was exploited in two different ways; the PVDF film is stretched out on a polyurethane support with a small curvature, or alternatively a hemicylindrical shape is imposed to the free sheet by clamping the narrowest sides along direction y at a distance of πr.

The piezoelectric equilibrium of a thin sheet of PVDF, polarized along the z or 3 direction and stretched along the x or 1 direction, is governed by the following equations:

$$S_1 = s_{11}^E T_1 + d_{31} E_3$$
$$D_3 = d_{31} T_1 + \varepsilon_{33}^T E_3$$

(5)

By applying an alternating voltage between the two electrodes, the hemicylindrical geometry and its lateral constraint allows the conversion of longitudinal motion into radial vibration (see Figure 6). Ultrasonic waves are generated in forward and backward directions. The resonance frequency is inversely proportional to the bending radius and can

be easily controlled by varying it. Neglecting the clamping effects, the resonance frequency is given by:

$$f = \frac{1}{2\pi r}\sqrt{\frac{1}{\rho s_{11}^E}} \tag{6}$$

where r is the radius of the curvature and $1/s_{11}^E$ and ρ are Young's modulus and mass density of curved PVDF film material, respectively (Fiorillo, 1992). Similar results were verified by finite element analysis (Toda, 2000). However in the curved geometry proposed by Toda and adopted by Hazas & Hopper (2006), clamping generates secondary acoustic fields which result in energy loss and directivity reduction.
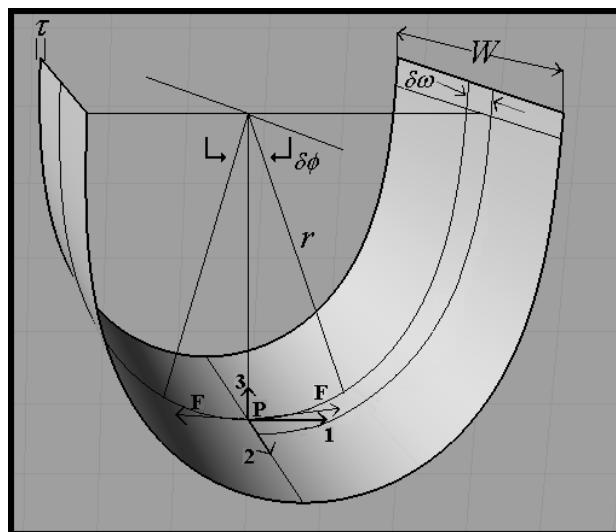
Fig. 6. A piezo-polymer film transducer obtained by curving a PVDF resonator in the length extensional mode along the 1 or stretching direction.

4.3 PVDF transducer modeling

Because of the ferroelectric polymer's inherent noise, a correct modeling of the transducer's electric impedance plays an important role in designing the electronic circuits. In order to design a specific electronic circuit capable of driving the PVDF transducer with high voltage over a wide band centered around the resonance, and of amplifying the echo with a high SNR (signal-to-noise-ratio), a Butterworth- VanDyke modified model has been implemented in the receiver. Both the modulus and the phase of the electric admittance of the transducer have been measured by using an impedance gain-phase analyzer.

Although the piezopolymer transducer suffers from high dielectric losses, the resonance frequency can be determined with good approximation from the phase diagram of the electric admittance. On the other hand, the almost flat diagram of the modulus around the resonance leads to more coarse results that, especially at low US frequency, need further manipulation in order to give reliable information. For instance, at the resonance frequency $f_r = 42.7 kHz$, the Butterworth-Van Dike modified model of the electric impedance of the transducer can be characterized by the following parameters: $R_s = 330 k\Omega$, $L_s = 10 H$, $C_s = 1.4 pF$, $R_0 = 210 k\Omega$, $C_0 = 248.5 pF$, where , R_0 has been introduced in the static branch to take into account dielectric losses as shown in Figure 7.
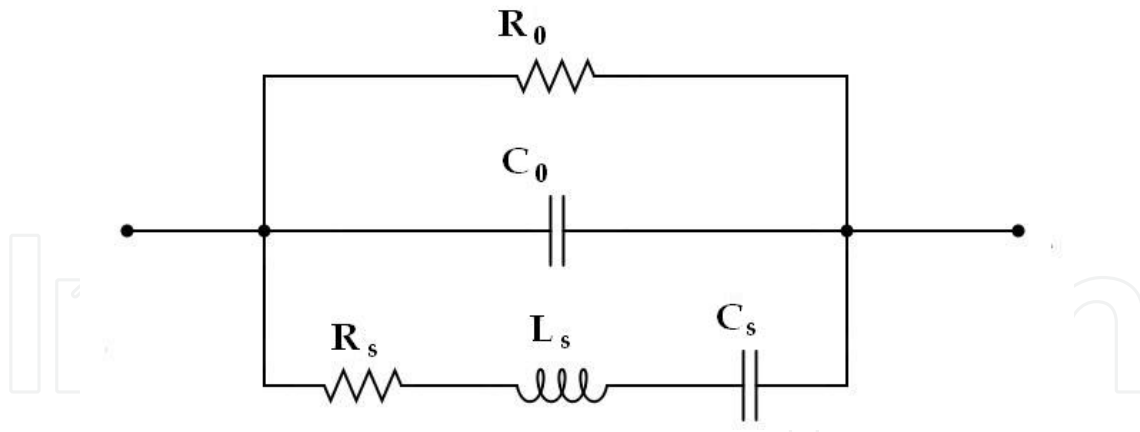
Fig. 7. Impedance equivalent model of the piezo-polymer transducer which also takes into account dielectric losses in which $R_0(\omega)$ and $C_0(\omega)$ are frequency-dependent parameters.

Piezoelectric devices are characterized by the figure of merit $M = k^2 Q$, where k is the electromechanical coupling and Q is the quality factor. In order to radiate or receive acoustical waves, piezoelectric transducers are required to have smaller M characterized by high k but low Q. Because of their inherent properties, piezo-ceramic and standard piezo-crystal sound transducers normally have high electromechanical couplings and high quality factors. We have modified the structure in order to increase the bandwidth and to further reduce the quality factor Q, while the resonance frequency can be continuously changed by modifying the film bending radius. As a result we obtained a controlled resonance transducer with a very low synthetic quality factor for choosing the right axial resolution and improving the pulse echo mode functioning over the full range frequency of bat biosonar (Fiorillo, 1996).

4.4 PVDF transducer with controlled resonance

In this second assembly, the transducer is realized by curving the sheet, according to parabolic shape, where the two extremities A and B, are tangentially blocked along two lines, t and t', that originate in point O (see Figure 8). The bending of the film is mechanically controlled by changing the opening arc angle ϕ between t and t'. The equation of the parabolic transverse section, $y = -ax^2 + c$, can be rewritten by considering two new parameters: the slope of t(t'), $m = \tan\left[(\pi - \varphi)/2\right]$ (m'=-m) , and d(d'), the fixed distance from the origin O to A (and B, respectively). Then, the arc length l has been evaluated as a function of d(d') and m(m'). Finally the ratio l/d (l/d') at various m(m') values, has been considered. Because of the imposed geometry and in order to assume a parabolic transverse section at any angular position ϕ, the ratio l/d (l/d') must be a constant quantity. Hence the film motion, converted from extensional to radial by geometry, can be studied by considering a parabolic shape in the range 27° < ϕ < 40° with an error less than 5%. When ϕ=50° the error increases up to 10%. By increasing the length l of the film in comparison with d(d'), it is possible to further increase the opening arc angle and, consequently, to reduce the resonance frequency. The transducer shape is now quite different from the parabolic one. However the maximum angle ϕ cannot exceed 70°, without the transducer being damaged.
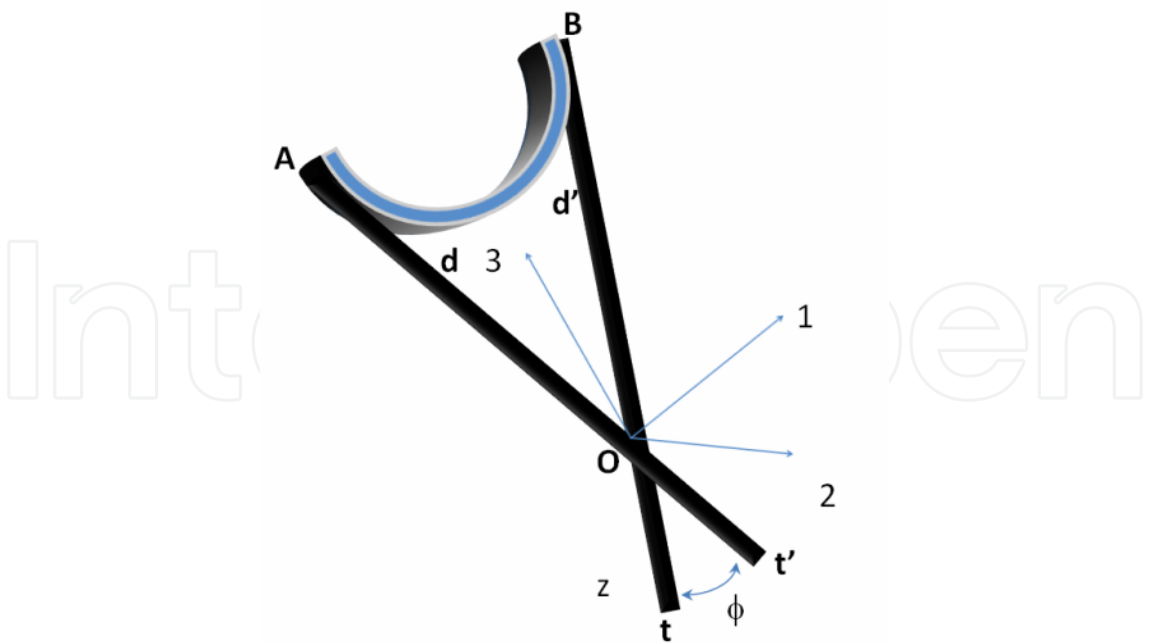
Fig. 8. Three dimensional view of transducer assembling in variable resonance frequency configurations clamped along A and B

ϕ [deg]	27	30	35	40	45	50	55	60	65	67
f_r [kHz]	65.1	61.3	54.6	50.5	47.3	42.7	38.0	35.8	34.3	30.0

Table 2. Resonance frequency vs opening arc angle

Experimental results show that the resonance frequency is inversely proportional to the opening arc angle ϕ between t and t'. It decreases from 65 kHz, when $\phi=27°$, to 45 kHz when $\phi=50°$. For $\phi>50°$ the film shape is quite different from a parabolic cylinder, however the resonance frequency decreases to 30 kHz by increasing the opening arc angle to $\phi=67°$. These results are in good agreement with previous results obtained using hemicylindrical transducers with circular transverse sections, different bending radii and different lengths.

By considering the upper -3dB frequency $f_H \approx 71.4$ kHz and the lower -3dB frequency $f_H \approx 27$ kHz (for each angular position it is $Q \approx 5$), when ϕ ranges, respectively, from 27° to 67° (see Table 2), a broad-band transducer $B=f_H-f_L=44.5$ kHz with central frequency of 49.25 kHz and very low synthetic quality factor $Q \approx 1$ is obtained.

The immediate advantage of this kind of transducer is the possibility of changing the axial resolution, which can be increased up to $\lambda/50$ (c/f, c=344 ms^{-1}, T=24 °C, relative humidity =77%) with digital phase measurement techniques of the transit time of the echo signal, and ranges between 250 μm, at $f_L \approx 27$ kHz , and 96 μm, at $f_H \approx 71.5$ kHz, for an accurate profile reconstruction up to a distance of 0.5 m. A closer dependence of the resonance frequency from both the bending radius and the opening arc angle, at different arc lengths, as well as a complete electromechanical model of the transducer, has been studied. This model takes into account the high dielectric losses of the piezo-polymer foil, even far from resonance.

Because the polymer's inherent noise also is related to its high dielectric losses, which are frequency dependent, as well as $C_0(\omega)$ and $R_0(\omega)$ (see Figure 7), we modified the parallel connection between C_0 and R_0 to have constant lumped parameters in the static branch over a broad frequency range.

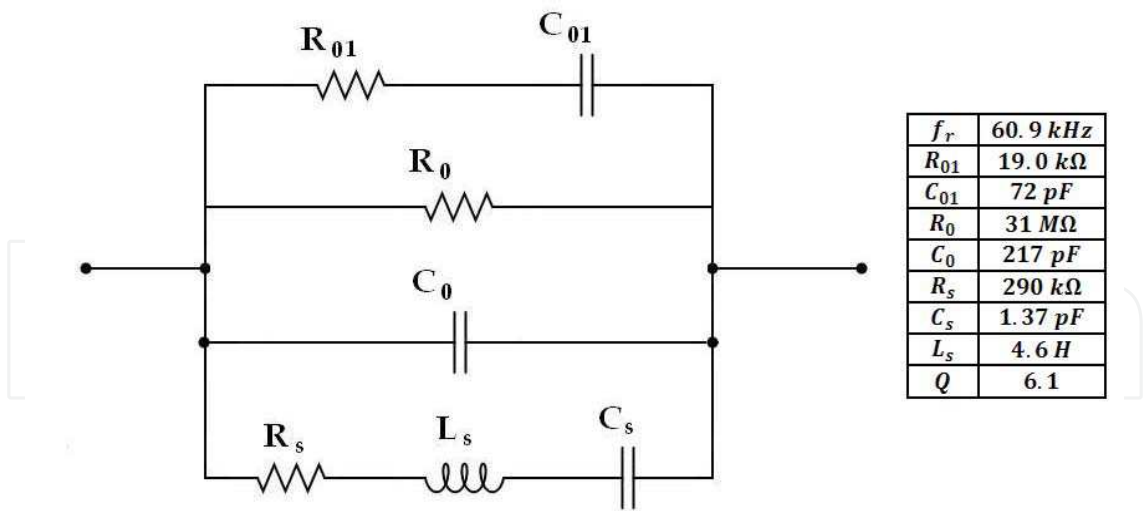| f_r	60.9 kHz
R_{01}	19.0 kΩ
C_{01}	72 pF
R_0	31 MΩ
C_0	217 pF
R_s	290 kΩ
C_s	1.37 pF
L_s	4.6 H
Q	6.1

Fig. 9. RLC equivalent electric circuit of the transducer in which the R C series branch makes the parameters independent of frequency variation in the range 1 kHz-150 kHz.

The static side of the equivalent electric circuit was modified by inserting a second branch that includes a resistor (R_{01}) connected in series to a capacitor (C_{01}) as shown in Figure 9. The values of C_0, R_0, C_{01}, R_{01} are approximately constant between 1÷150 kHz. The electric behavior of the two static networks was equivalent in the frequency range of interest. In addition the modified equivalent admittance better approximates the measured values (Fiorillo, 2000). Once we determined the equivalent electrical circuit with constant electric parameters, of the lossy transducer in a relatively broad frequency range, we investigated the pre-amplifier noise sources and the noise generated in the receiver, Rx, to optimize SNR. For this reason we took into account the transducer equivalent electric network with related Johnson noise sources. We did not consider noise sources in the transmitter, Tx, because the driving voltage can be arbitrarily increased within the limits of dielectric breakdown.

5. Echo-location techniques of bat

There are 966 species of bats that use different ultrasonic waveforms to move between obstacles and to locate the target. The most simple bio-pulses are very simple clicks of around 40 kHz. Some species emit constant frequency signals, CF, a sinusoidal burst of many cycles, or frequency modulated signals, FM. Another more sophisticated form of the US signal is a combination of a CF pulse immediately followed by a downward chirp, an FM pulse. This kind of CF-FM, can be a pure tone or a multi-harmonic signal. Its energy may be selectively controlled depending on the distance and the size of the target.

5.1 Echo-location of Pteronotus Parnellii

The most complex CF-FM pulse is that emitted by the Pteronotus Parnellii, or moustached bat, which is composed of four harmonics: the fundamental CF_1-FM_1, at 30.5 kHz, followed by the downward chirp in which the frequency is reduced to 20 kHz, and three higher harmonics, followed by relative chirps, CF_2-FM_2 at 61 kHz, CF_3-FM_3, at 92 kHz, and CF_4-FM_4 at 123 kHz respectively down to about 50, 80, and 110 kHz (see Figure 10a). The mustached bat is able to extract plenty of information from the echo signal as shown in Figure 10b.

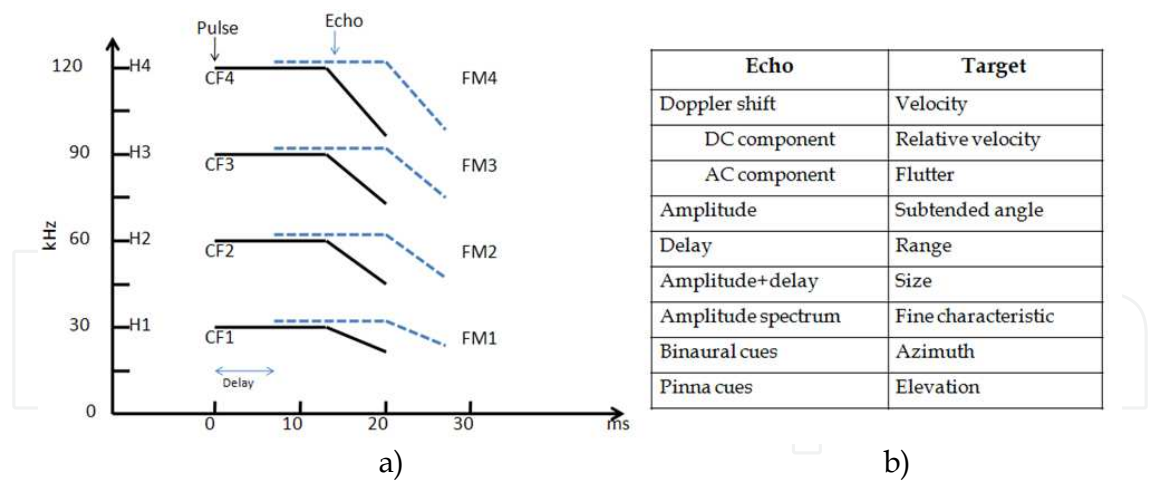a)   b)

Fig. 10. The four pulse components of the bio-signal generated by the mustached bat. In diagram a) the solid line represents the superimposed CF-FM component, while the dashed line depicts the received echo . Table b) shows information received by the bat related to the characteristics of the echo signal analysis.

Distance is evaluated using the echo delay, throughout the time-of-flight (TOF) as related to the frequency modulated components FM_2, FM_3, FM_4. The FM signals are used to cover the whole range of the bio-sonar. In particular the components FM_2, FM_3, FM_4 operate at the maximum, medium and minimum distance, while the first component, FM_1, is used to start the TOF measurement and is sent to the auditory system, internally, through the larynx. A neural network model based on FM-FM neurons and proposed by Suga (1990) is shown in Figure 11. The neural network is mainly divided into two parts:

- An afferent pathway appointed to the transmission of the PFM_1 pulse
- An afferent pathway appointed to the reception of EFM_n (n=2, 3 or 4) echoes
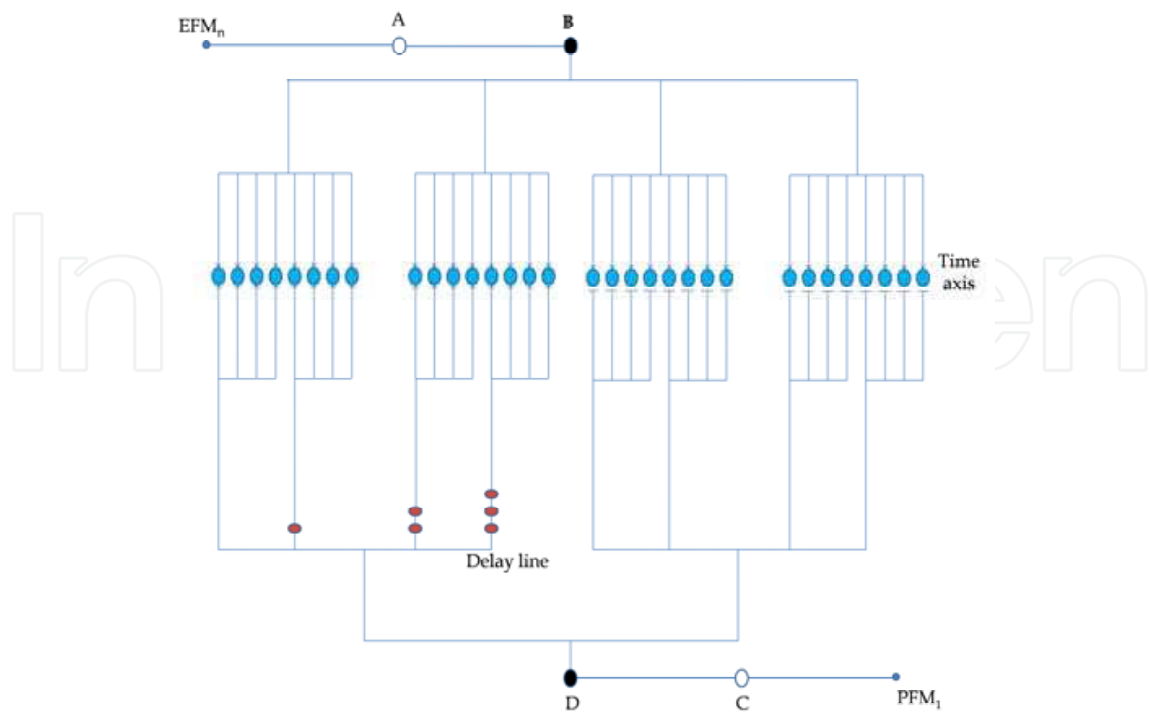
Fig. 11. Scheme of a portion of the neural network for ranging analysis

The neural network compares the first component PFM_1 with each one of the other three EFM_2, EFM_3 and EFM_4, in three different neural structures: one for PFM_1-EFM_2, one for PFM_1-EFM_3 and one for the PFM_1-EFM_4 components. The FM_n (n=2,3 or 4) components of the echo are elaborated by the neural network in order to obtain a sequence of bio-pulses, each one related to a particular delay time. The neurons are located over the delay time axis and are tuned to a particular delay time from 0.4 ms to 18 ms. They receive the echo naturally delayed by the target from the upper network (neurons EFM_n, A, B). This echo reaches all the neurons of the time axis. Similarly the start pulse (PFM_1) reaches each neuron of the time axis from the lower network (neuron PFM_1, C, D) with increasing delay accomplished either with variation in length and axon diameter or by different time inhibition values. In this neural structure only one neuron is excited, by both EFM_n and PFM_1, when the echo and the pulse are combined with a particular delay, and generates an action potential at the time-of-flight as related to target distance.

5.2 The PVDF sonar system and the afferent electronic pathway

The PVDF transducer can be used as a transmitter (converse piezoelectric effect) or a receiver (direct piezoelectric effect) of ultrasonic signals. The circuit for driving the transmitter with CF – FM signals, is realized using a power operational amplifier, followed by a step-up transformer, that generates a wide range of signals from a few volts up to a few hundred volts in both CF and FM mode. The receiver converts ultrasonic energy into electric energy and the signal is firstly pre-amplified with a very low-noise, low-distortion operational amplifier, designed for low frequency ultrasound applications (Fiorillo et al., 2010). It is then filtered and conditioned to be suitable for neural network processing as shown in Figure 12.
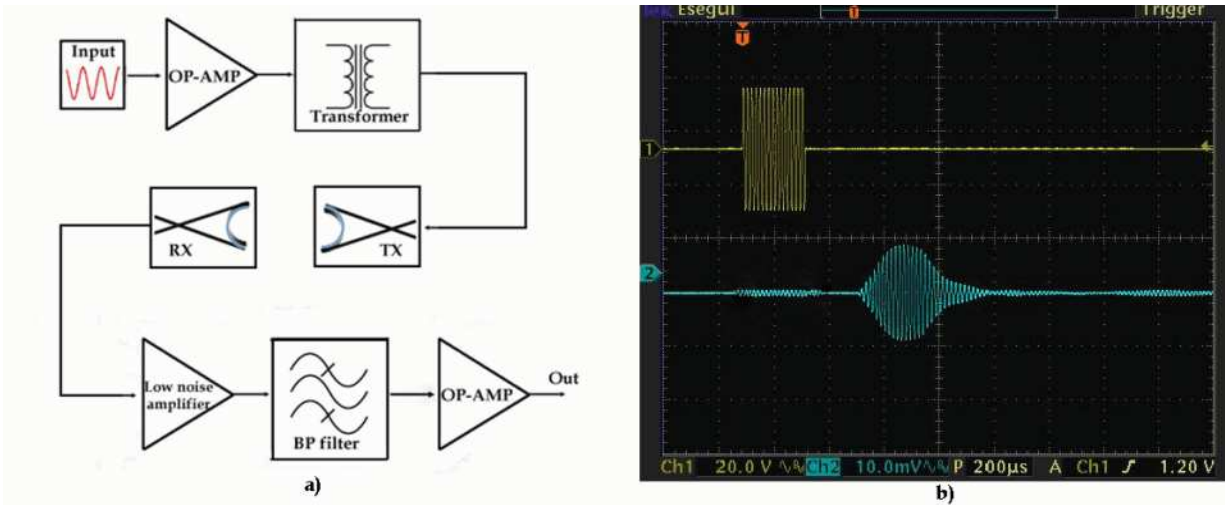

Fig. 12. Block diagram of the transmitter and receiver circuit a). 65 kHz burst signal (upper) reflected by a plane (lower) located at 150 mm from the sonar b).

The first step is to create a sequence of suitable pulses, each related to a particular frequency of the FM signal, in order to evaluate the TOF. For simplicity, the FM_2 echo component and the related neural network will be considered. The FM_2 signal is a down-chirp from 65 kHz to 49 kHz with a duration of about 6 ms, from which a sequence of suitable pulses is created to activate the artificial neural network.

In the electronic system the pulse sequence related to the spectral components is obtained by filtering and then rectifying the FM_n (n=2…4) signals. Finally the signal is again filtered at low frequency to extract the envelope shown in Figure 13.
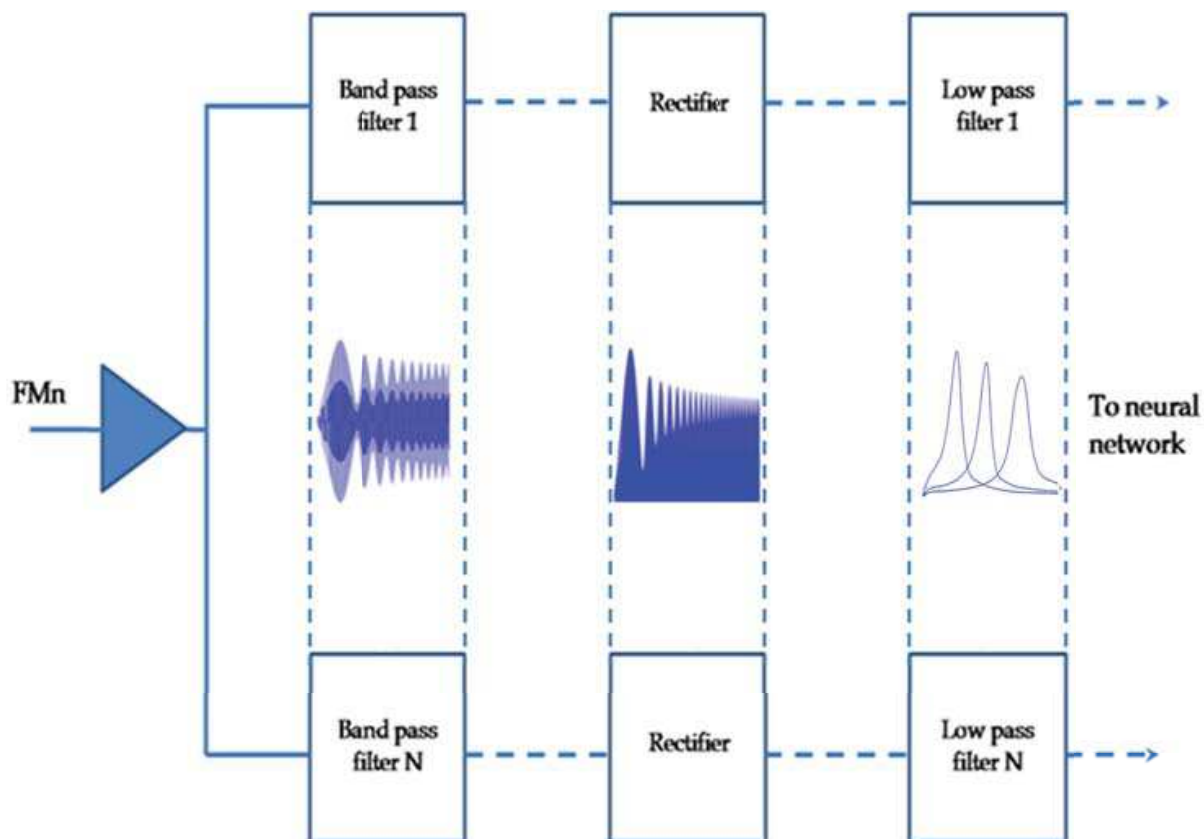

Fig. 13. Schematic simulation of cochlea signal conditioning

These pulse signals are sent in parallel to the neural network which compares the first component PFM_1 with each one of the other three EFM_2, EFM_3, EFM_4 in three different neural structures: PFM_1-EFM_2, PFM_1-EFM_3 and PFM_1-EFM_4.

Similarly PFM_1 is converted in a sequence of pulses according to a time-frequency correspondence. In fact, when both PFM and EFM signals reach the neural network as a pulse sequence, frequency losses sense since it is related to the particular delayed pulse. According to the Suga model, neurons A and C respond to the stimulus with action potentials, while in our electronic system voltage pulses are sent, from neurons A and C through neurons B and D, in the afferent ways, to the time axis.

In Figure 14 one can see the neural network learned and simulated in Matlab in which only three neurons A (C) and four FM-FM neurons along the time axis are considered, for simplicity's sake. The A neurons, which receive the output signal from the block diagram shown in Figure 13, are implemented by using a multilayer perceptron structure trained with a back propagation algorithm. It reduces the envelope duration around its peak value (see Figure 15) in order to improve the cross-correlation analysis performed by the FM-FM neurons.

The neural model offers a possible description in terms of cross-correlation analysis according to signal codification and time of flight detection as in bat biosonar for ranging evaluation.
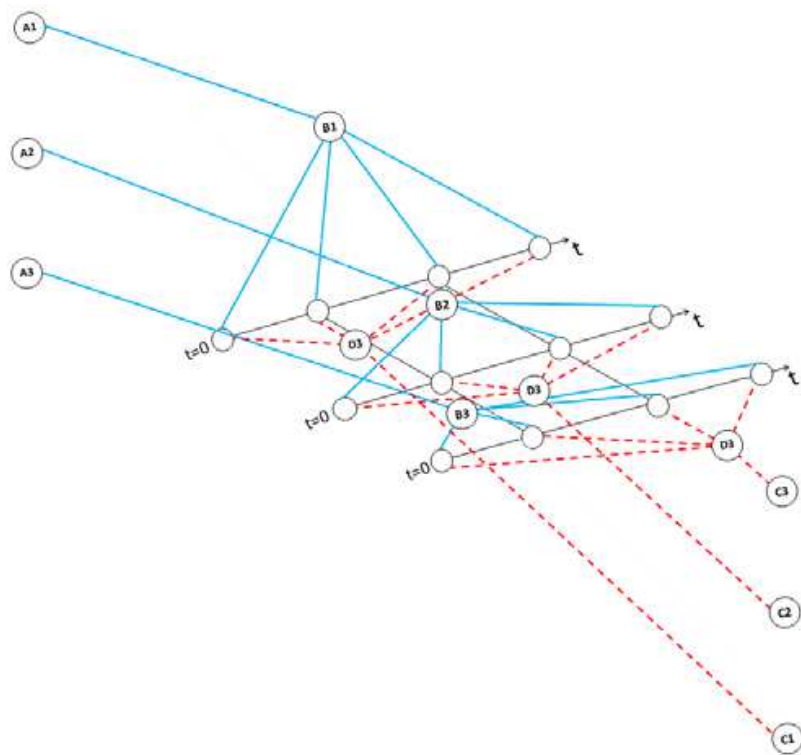
Fig. 14. Portion of a three-level neural network in which each neuron A (or C) receives the corresponding envelope that is sent through neurons B (or D) to FM-FM neurons
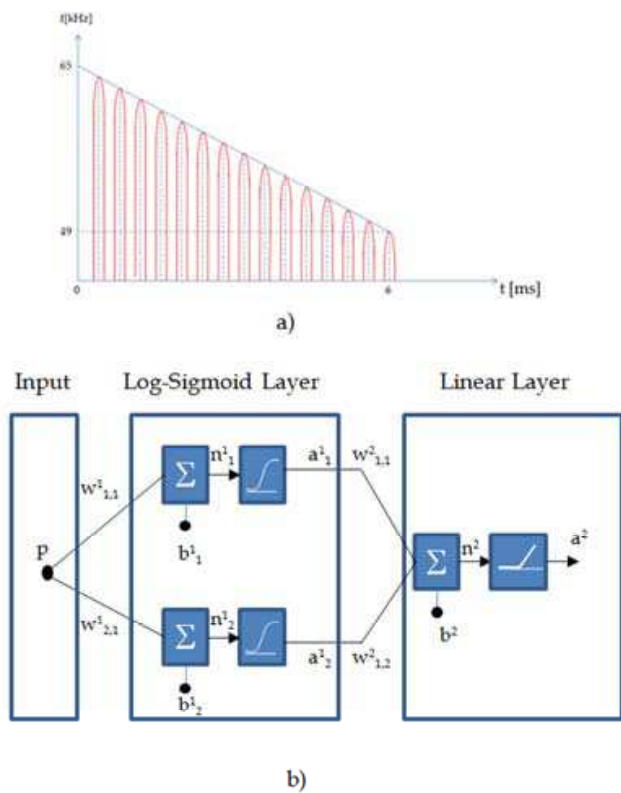

Fig. 15. a) Sequence of 16 pulses, related to a 16 echo envelope, at the output of A neurons. b) Neuron multilayer perceptron implemented in Matlab environment

6. Conclusion and future development

It is our opinion that ferroelectric polymer-based sensors for low frequency ultrasound in air represent the best compromise between versatility and performance.

In effect, the curved PVDF ultrasonic transducer is the only one capable of resonating over a wide frequency range. In fact, the functioning of the majority of standard or custom transducers, based on different technologies, is limited to narrow frequency bands which reduce their use to a restricted field of application. For this reason most research is concerned with signal processing rather than transducer technology. The efficiency of ultrasonic transducers is clearly improved by the ferroelectric polymer technologies. PVDF transducers can adapt work modalities to tasks almost in medium range application in air according to strategies observed in the flight of bats.

Our work shows the possibility of using PVDF transducers to replicate the behaviour of bat bio-sonar despite the fact that only ranging was considered. Future developments must be concerned with the implementation of suitable neural networks for the explication of different tasks as relative to velocity, target size and finer characteristics. All of these problems could be approached in terms both of technology and of neural networking.

7. References

Altringham, J. (1986). *Bats: biology and behavior*. Oxford University Press, New York

Bauer, F. (1986). Method and device for polarizing ferroelectric materials, *U.S. Patent 4,611,260*, USA

Bergman, J.G., McFee, J.H., Crane, G.R. (1971). Pyroelectricity and optical second harmonic generation in polyvinylidene fluoride films, *Applied Physics Letter*, Vol. 18, No. 5, pp. 203-205, 0003-6951

Berlincourt, D. (1981). Piezoelectric ceramics: characteristics and applications, *Journal of the Acoustical Society of America*, Vol. 70, No. 6, pp. 1586-1595, 0001-4966

Bloomfield, P.E., Marcus, M.A. (1988). Production of ferroelectric polymer films, In *Applications of Ferroelectric Polymers*, Wang, T.T., Herbert, J.M., Glass, A.M., Blackie & Son Ltd, Chapman and Hall, New York

Brown, L.F., Carlson, D.L. (1989). Ultrasound transducer models for piezoelectric polymer films, *IEEE Transaction on Ultrasonics, Ferroelectrics and Frequency Control*, Vol. 36, No. 3, pp. 313–318, 0885-3010

Davis, G.T. (1988). Structure, morphology, and models of polymer ferroelectrics, In *Applications of Ferroelectric Polymers*, Wang, T.T., Herbert, J.M., Glass, A.M. Blackie & Son Ltd, Chapman and Hall, New York

De Condillac, E.B. (1754). *Condillac's treatise on the sensations*, Geraldine Carr (trans.), Favil Press, London

Hasegawa, R., Takahashi, Y., Chatani, Y., Tadokoro, H. (1972). Crystal structure of three crystalline forms of poly(vinylidene fluoride), *Polymer Journal*, Vol. 3, pp. 600-610

Hasegawa, R., Kobayaschi, M., Tadokoro, H. (1972). Molecular conformation and packing of poly(vinylidene fluoride). Stability of three crystalline forms and the effect of high pressure, *Polymer Journal*, vol. 3, No.5, pp. 591-599

Hunt, J.W., Arditi, M., Foster, F.S. (1983). Ultrasound transducers for pulse echo medical imaging, *IEEE Transaction on Biomedical Engineering*, Vol. BME-30, No. 8, pp. 453-481, 0018-9294

Jona, F, Shirane, G. (1962). *Ferroelectric crystals*, Pergamon Press, New York

Fiorillo, A.S. (2000). Noise analysis in air-coupled PVDF ultrasonic sensors, *IEEE Transaction on Ultrasonics, Ferroelectrics and Frequency Control*, Vol. 47, No.6, pp. 1432-1437, 0085-3010

Fiorillo, A.S. (1996). Ultrasound transducer with low synthetic quality factor, *Applied Physic Letters*, Vol. 68, No. 2, pp. 164-166, 0003-6951

Fiorillo, A.S., Design and characterization of a PVDF ultrasonic range sensor, *IEEE Transaction on Ultrasonics Ferroelectrics and Frequency Control*, Vol. 39, No. 6, pp 688-692, 0085-3010

Fiorillo, A.S., Van der Spiegel, J., Esmail-Zandi, D., Bloomfield, P.E. (1990). A P(VDF/ TrFE) based integrated ultrasonic transducer, *Sensors and Actuators A: Physical*, Vol. 22, No.1-3, pp. 719-725, 0924-4247

Fiorillo, A.S., Lamonaca, F., Pullano, S.A. (2010). PVDF based sonar for a remote web system to control mobile robots, *Sensors & Transducers Journal*, Vol. 8, Special Issue, pp. 65-73, 1726-5479

Hazas, M., Hopper, H. (2006). Broadband ultrasonic location systems for improve indoor positioning, *IEEE transaction on Mobile Computing*, Vol. 5, No. 5, pp. 536-547, 1536-1233

Lewin, P.A., De Reggi, A.S. (1988). Short range applications, In *Applications of Ferroelectric Polymers*, Wang, T.T., Herbert, J.M., Glass, A.M. Blackie & Son Ltd, Chapman and Hall, New York

Lovinger, A.J. (1983). Ferroelectric polymers, *Science*, Vol. 220, No. 4602, pp. 1115-1121

Lovinger, A.J. (1982). Developments in crystalline polymers, *Applied Science*, Vol. 1, No.5

Mason, W.P. (1981). Piezoelectricity, its history and applications, *Journal of the Acoustical Society of America, Vol. 70*, No. 6, pp. 1561-1566

Mason, W.P. (1964). *Piezoelectric crystals and their applications to ultrasonic*, Van Nostrand Company, Inc. 4th ed., New York

Sessler, G.M. (1981). Piezoelectricity in polyvinylidenefluoride, *Journal of the Acoustical Society of America,* Vol. 70, No. 6, pp. 1596–1608

Swartz, R.G., Plummer, J.D., Integrated silicon-PVF2 acoustic transducer arrays, *IEEE Transaction on Electron Devices*, Vol. 26, No. 12, pp 1921-1931, 0018-9383

Suga, N. (1990). Cortical computational maps for auditory imaging, *Neural Networks*, Vol.3, No. 1, pp.3-21, 0893-6080

Toda, M., Tosima, S. (1999). Theory of curved clamped PVDF acoustic transducers, *Proceeding of IEEE Ultrasonic Symposium*, 1051-0117, Caesars Tahoe, October

Wang, H., Toda, M. (1999). Curved PVDF airborne transducer, *IEEE Transaction on Ultrasonics Ferroelectrics and Frequency Control*, Vol. 46, No. 6, pp. 1375–1386, 0885-3010

Yamaka, E., Teranishi, A. (1977). Pyroelectric Vidicon Tube with PVF, Film and Its Application, *Proceeding of the 1st Meeting on Ferroelectric Materials and Their Applications*, Kyoto, November
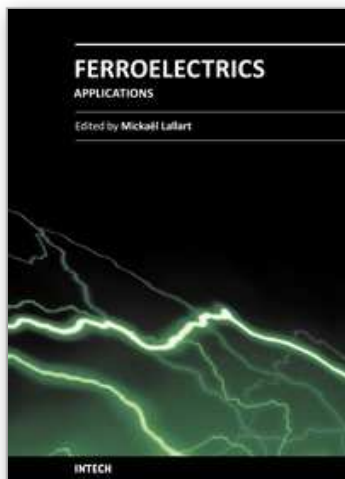
Ferroelectrics - Applications

Edited by Dr. Mickaël Lallart

Ferroelectric materials have been and still are widely used in many applications, that have moved from sonar towards breakthrough technologies such as memories or optical devices. This book is a part of a four volume collection (covering material aspects, physical effects, characterization and modeling, and applications) and focuses on the application of ferroelectric devices to innovative systems. In particular, the use of these materials as varying capacitors, gyroscope, acoustics sensors and actuators, microgenerators and memory devices will be exposed, providing an up-to-date review of recent scientific findings and recent advances in the field of ferroelectric devices.

How to reference

In order to correctly reference this scholarly work, feel free to copy and paste the following:

Antonino S. Fiorillo and Salvatore A. Pullano (2011). Ferroelectric Polymer for Bio-Sonar Replica, Ferroelectrics - Applications, Dr. Mickaël Lallart (Ed.), ISBN: 978-953-307-456-6, InTech, Available from: http://www.intechopen.com/books/ferroelectrics-applications/ferroelectric-polymer-for-bio-sonar-replica

INTECH
open science | open minds